Sustainable Reactive Powder Concrete Incorporating Industrial Wastes: Mechanical and Durability Assessment under Variable Curing Regimes

S. Revathi[1*], D.Brindha[2]

[1] Department of Civil Engineering, Mepco Schlenk Engineering College, Sivakasi, srevathi@mepcoeng.ac.in
[2] Department of Civil Engineering, Thiagarajar College of Engineering, Madurai, dbciv@tce.edu
[*] Corresponding author, E-mail: srevathi@mepcoeng.ac.in

Graphical Abstract

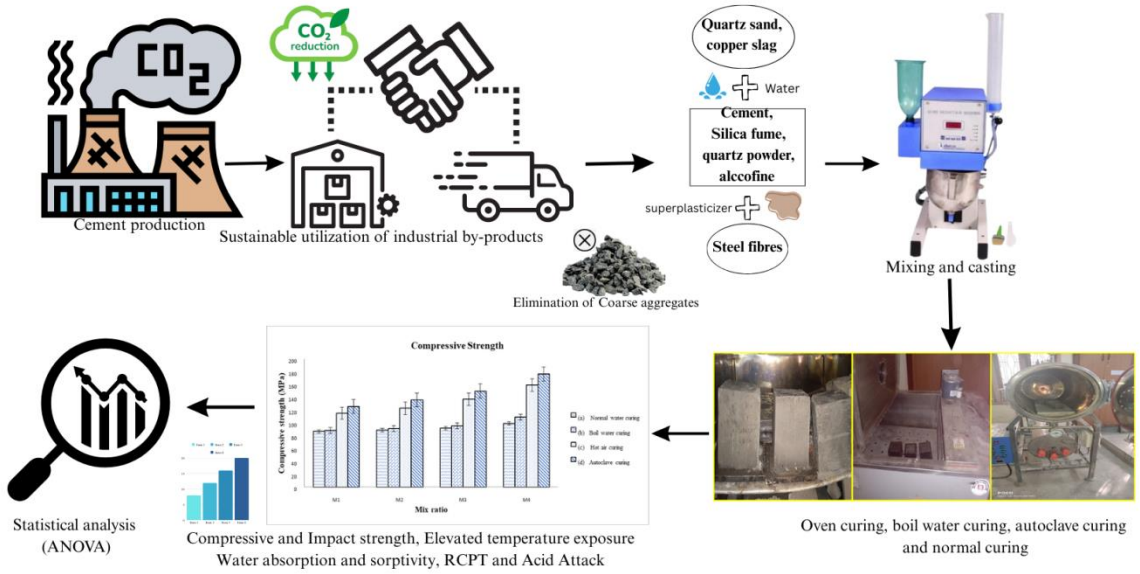

Abstract

Cement production significantly contributes to global carbon dioxide emissions; in Reactive Powder Concrete (RPC), incorporation of sustainable by-products and elimination of coarse aggregate reduces emission, improves particle packing, and enhances strength, echoing the shift from normal concrete to Ultra-High-Performance Concrete (UHPC). Among them, foremost is RPC, which is made of fine particles such as quartz sand, quartz powder, and cementitious materials such as silica fume, cement, admixtures, and fibres, which improves ductility. This research investigates the mechanical properties like compressive strength and impact strength and durability properties like water absorption, water sorptivity, acid attack, chloride penetration, and residual compressive strength under elevated temperatures of 300 °C, 600 °C,

and 900 °C. This paper also examines the effectiveness of various curing conditions and adding cementitious materials to enhance RPC. The various curing conditions taken for the study are water curing, boil water curing, autoclave curing, and oven curing. The test results show a compressive strength of 176.5±0.62 MPa was achieved in RPC by replacing 10 % cement with Alccofine and 40 % quartz sand with copper slag under autoclave curing. Also, the significant effect of mix ratios and curing conditions on the strength of concrete is done by ANOVA analysis. The results suggest that the mixes with high cement and pozzolonic content under the autoclave curing method yield the strongest material. This research aligns with sustainable goals such as SDG 9: Industry, Innovation, and Infrastructure; SDG 11: Sustainable Cities and Communities; and SDG 12: Responsible Consumption and Production.

Keywords: Reactive Powder Concrete (RPC), alccofine, copper slag, industrial wastes, mechanical and durability properties, sustainability, curing, elevated temperature, ANOVA.

1. Introduction

The growth of India's economy is directly correlated to the country's progress in infrastructural development. Infrastructure development must be carried out in an eco-friendly aware, responsible and sustainable manner because construction is the country's second major economic contributor (around 9%), behind agriculture [Muhedin & Ibrahim, 2023]. Cement, which is the most crucial material, is also one of the key manufacturers of CO_2 and a contributor to greenhouse gas. High cement content can have unfavourable consequences on production costs, heat of hydration, and, potentially, shrinkage issues. A possible answer to these issues is to use mineral admixtures in place of cement [Al Biajawi, et.al., 2022]. Over the last few years, researcher's efforts to improve the performance of concrete have demonstrated that supplemental cementitious ingredients with mineral admixtures may boost the strength and longevity of structure [Wu, et.al., 2022, Fallah-Valukolaee, et.al., 2022, Nguyen, et.al., 2025]. The utilization of alternative cementitious materials can reduce the massive energy expenditure and CO_2 emission rate associated with cement production for concrete. [Zhang, et.al., 2024, Gao,

et.al., 2024] By replacing a portion of the cement in binary or even ternary blended concrete with these elements, the problem of waste disposal can be mitigated, and hundreds of millions of tonnes of by-product materials can be used [Jalalinejad, 2023]. The last two decades have seen remarkable advancements in concrete technology, made possible by a new formulation method based on the use of ultra-fines components and supported by the robust development of novel admixtures such as sugarcane bagasse ash [Rajasekar, et.al, 2018a, 2019], alccofine, fly ash [Huynh, et.al., 2024] and powders from waste glass bottles and ceramic tiles [Radhi, et.al., 2021], granulated blast furnace slag and rice husk ash [Ahmed, 2024]. Nasr, et.al., (2021) also explored the possibility of using Treated-Bagasse Ash (TBA) in place of cement and found that 15 % replacement ratio was optimal, with improved performance and no negative effects on the hardened concrete. There is a rising interest in Reactive Powder Concrete (RPC) which was created by scientists at the France laboratory and patented by Richard and Cheyrezy in 1994. RPC consists of ultra fine powders such as cement, silica fume, quartz sand and quartz powder where cement undergoes hydration, silica fume enhances pozzolanic behaviour with the resulting calcium hydroxideformation (CH), quartz sand supplies silica for the development of additional Calcium-Silicate-Hydrate (C-S-H) gel, and quartz powder modifies the Calcium Oxide to Silicon dioxide (SiO_2) ratio to improve the formation of tobermorite structure. All of these powder components chemically react and create dense packing which increases the strength of concrete. In order to speed up the siliceous activity of quartz, which modifies the microstructure behaviour of RPC, and to eliminate any surplus water, RPC must be subjected to heat treatment after setting. With steel aggregate added to the mixture of RPC, ultra-high strength can be achieved. This cement-based fibre-reinforced composite material improves the strength and durability of RPC. The density of cement in RPC typically exceeds 900 kg m^{-3}. Several materials such as waste glass powder, waste fly ash, phosphorous slag powder, sugarcane bagasse ash, ground granulated blast furnace slag (GGBS) were used by the researchers to replace a portion of cement in RPC [Abed and Nemes, 2019, Jalalinejad, et.al.,

2023, Chen, et.al., 2023, Banerji, et.al., 2024] . The partial replacement of cement with fly ash and silica fume reduced CO_2 in the atmosphere by 12-25% based on mix design [Moolchandani, 2025] Another cement replacing material such as alccofine 1203 is an ultrafine material derived from GGBS which is perfectly suitable for RPC because of its size and composition. Using a regulated granulation process, the Alccofine 1203 achieves a high degree of reactivity in addition to its high glass content. Alccofine-1203's calcium and silicon content makes it more effective than other ingredients at enhancing concrete's mechanical and durability attributes. The researchers found that alccofine achieved more strength than standard concrete for a lower cost, hence they proposed it for use in the Indian building industry [Mir & Kumar, 2024, Durai, et.al., 2025]

Researchers also focused on improving the ductility and toughness of RPC with various fibres such as steel fibres, carbon fibres and basalt fibres [Raza,, et.al., 2021, Ge, et.al., 2023, Salahaddin, et.al., 2024]. But when adding fibres to the concrete, flow value gets reduced. Fibre added at 0 % to 1.0 %, 2.0 %, and 3.0 % with 30 % addition of silica fume increased compressive strength by 20 %, 26 %, and 41 %. Fibre content addition in RPC increased the tensile strength and flexural strength [Abd El Raheem, et.al., 2020]. Researchers found that Recycled Steel Fibres (RSF) from recycled tyres helps control the carbon footprint of fibre-reinforced concrete. The findings of the tests indicated that adding 3 % RSF enhanced the crushing strength, tensile strength and flexural strength values of plain-RPC by 9 %, 23 %, and 58 %, respectively [Rajasekar, et.al., 2018b, Raza, et.al., 2022]. Salman et al., (2018) inferred that ductility was needed for concrete to increase its breaking strength and strain hardening. Close-spaced micro steel fibres strengthened concrete and reduced cracks. Compared to other cement, the mix with 100 % OPC exhibited better shrinkage resistance and mechanical properties. Mizani, et.al., (2022) examined the impact of fibre quantity and fibre type on the mechanical features of RPC, and compared the mixing procedures used to achieve their goals. Experimental results indicated that hybrid (macro and micro) steel fibres added at a rate of 1.5 %

had a major beneficial effect on improving the mechanical characteristics of RPC. The results showed that incorporating 0.5 % fibres into RPC did not substantially improve the material's mechanical characteristics [Zhang, et.al., 2019]. In their work, they inferred that incorporating micro-steel fibre of length 6mm and of diameter 0.6 micron postponed the cracking while applying load. Waste aggregates and waste fibers were added, and the RPC was named Green Reactive Powder Concrete [Atlı & Ipek, 2024]. Recycled steel fibers from waste tyres showed similar results compared to industrial steel fibers [Hasan, 2024]. The optimal and economical mix design with straight and hooked fibers was designed by Artificial Neural Network (ANN) and enhances the sustainable construction process [Naveed et al., 2025].RPC's mechanical and durability qualities are affected by curing procedures and cement quantity. Chen, et.al., (2023), explored that early mechanical strength of UHPC was achieved at heat curing with 90°C, whereas the mechanical properties were damaged at high pressure and temperature of 2MPa and 250°C. But the hydration and pozzolanic reaction occurred in steam and autoclave curing. Lessly, et.al, (2021) examined UHPC long-term behaviour and its mechanical characteristics. With accelerated curing, compressive strength reached 180.9 MPa, a 30 % increase. Steam curing improved concrete thickness from 0.2 % to 1 % after 28 days of sulphate attack, compared to the other two curing regimes such as normal and heat curing [Hiremath & Yaragal, 2017a]. Fibres delay micro-cracks in the concrete, increased cyclic loading and flexural characteristics, and prevent sudden failure. High temperature curing created cementitious particles with a lower Calcium-Silicate (C/S) ratio and accelerated secondary hydration reaction [Chen, et.al., 2019]. Abid , et.al., (2025) explored the RPC's strength and structural integrity using standard room curing, steam curing, hot temperature curing and concluded that high temperature curing increased RPC's mechanical performance. Hendi & Aljalawi (2024) inferred that the increase in compressive strength and flexural strength occurred by using warm water curing at 35°C. Mayhoub, et.al., (2021) inferred that autoclave curing and low cement dose produced high compressive strength than steam curing and also they inferred that Fly ash with

40 % replacement of cement under autoclaving increased compressive strength by 33 % and rice husk ash with 30 % replacement of fumed silica under steam treatment enhanced the compressive strength by 45 %. Mostofinejad, et.al., (2016) mentioned that combined curing (Autoclave curing- 3 days at 125 °C with heat curing- 7 days at 220 °C) gave superior mechanical properties.

The production technique of RPC is fuzzy since numerous parameters affect its fresh and hardened properties. Mixing techniques, speed of mixing, and mixing duration also affect fresh qualities for the same composition [Hiremath & Yaragal, 2017b]. Researchers inferred that greater mixing speed and duration reduced RPC flow and strength. Due to the hydration processes, all concrete, regardless of the curing method, dried out and shrank on its own; however, the degree of autogenous shrinkage changes depends on the mix proportions [Abed & Nemes, 2019]. The lower shrinkage strain was observed in HPC reinforcing with fibers than the HPC without fibers and shrinkage reduction occurred when increasing steel fiber content. [Hongthong, et.al., 2025]. The drying and autogenous shrinkage is reduced by adding water reducing agent as reported by Feng, et.al., 2025. As the world's supply of high-quality natural sand continues to dwindle, there has been a rise in the number of studies considering the viability of utilizing industrial waste products as a suitable substitute. Hameed, et.al., (2024) used the hybrid aggregate recycled concrete produced from construction and demolition waste to improve the compressive strength and durability of concrete.. The manufacturing of both copper and pig iron generates by-products called Copper Slag (CS) and Blast Furnace Slag (BFS), respectively [Ojha, et.al., 2021]. They used copper slag, blast furnace slag and air-cooled blast furnace slag as a replacement for natural sand and different mechanical characteristics and durability-related criteria of them were studied. For many years, CS from copper industry was used as replacement for natural fine aggregate in concrete to make the concrete denser and impermeable. Hence, fewer natural resources are used, and the copper company has less adverse effect on the environment.

As cement content improves, so does the variation in RPC's compressive behaviour. RPC requires a lot of cement; however, it can be supplemented by mineral admixtures. In this work, alccofine 1203 was used for replacing cement and CS was used to replace quartz sand. When compared to conventional curing, the mechanical property of RPC that was treated by heat and steam was significantly more extensive**.** In this work, water curing, steam curing, heat curing and autoclave curing of RPC had been studied in terms of its effect on the material's mechanical qualities. The effects of all four types of curing on mechanical strength and durability of concrete have also been studied. Properties of RPC were significantly impacted by all four curing conditions. The autogenous shrinkage caused by hydration was mitigated by thermal expansion. Under actual in-situ conditions, the combined effect of the two may have a considerable impact on the concrete deformations. Significant consequences, such as the volumetric conflict between hardened concrete and cracking partially or entirely, may result from excessive autogenous shrinkage.

Although numerous studies have investigated the behaviour of RPC under various curing conditions, limited work has been done on the combined effect of alccofine and copper slag on the strength and durability properties, mainly under various accelerated curing conditions such as autoclave curing and hot air curing. Moreover, the inclusion of industrial wastes in RPC remains insufficiently explored. This research aims to create a sustainable reactive powder concrete by incorporating industrial by-products such as silica fume, quartz powder, alccofine and copper slag and to evaluate the mechanical and durability properties of RPC under four curing conditions (normal water, boil water, hot air and autoclave curing) thereby making it relevant for infrastructural applications exposed to aggressive environments. The research focuses on reducing cement content by reuse of industrial waste materials and enhancing the performance of concrete, thereby addressing both environmental and engineering challenges.

2. Materials

The process of raw material selection in adequate proportions and quality is essential for RPC to achieve its required strengths. The combined use of the materials chosen results in an ultra-dense matrix, which improves both strength and durability, while simultaneously promoting sustainability by effectively utilizing industrial waste materials.

***2.1 Cement, Silica fume and quartz sand*:** The cement used in this work was Ordinary Portland Cement (OPC) grade 53. The specific gravity of cement was 3.10, its initial and final setting times were 35 minutes and 610 minutes, respectively, and its consistency was 28 %. The silica fume used in this study was a white-coloured micronized powder with a specific gravity of 2.64, and it was composed of 99.92 % silica and trace amounts of alumina and ferric oxide. The quartz sand used in this study was white in colour and it had 99 % silicon dioxide content and trace amounts of metal and iron oxide.

2.2 Quartz powder: When combined with cement and silica content, this powder behaves as filler between the larger particles. Its chemical and thermal qualities make it a vital ingredient in making a material that is very strong, durable, and wear-resistant, and its usage as an additive helps to improve the density and minimize the vulnerability of the concrete. The quartz powder used in this study was a white-coloured fine powder with a specific gravity of 2.60 and had 99.50 % silicon dioxide and trace amounts of alkalies and oxides.

2.3 Alccofine: Alccofine's main benefit as a component of RPC is in enhancing the concrete's workability. Alccofine-1203 is prepared from GGBS, which is the waste material from iron ore industries by several processes. It is a fine powder that creates good particle packing of ultrafine particles having a unique chemical composition and reduces the water and admixture dosage. The characteristics of alccofine used in this study was grey in colour with a specific gravity of 2.80, and it had 30-34 % of calcium oxide, 30-36 % of silicon dioxide, 18-25 % of aluminum oxide, 1.8-3 % of iron oxide, and 6-10 % of magnesium oxide.

2.4 Copper Slag and Steel fibre: The copper slag used in this study was blackish grey in colour and it had 40-44 % iron, 33-35 % silicon dioxide, 4-6 % aluminum oxide, and trace amounts of copper, calcium oxide, and magnesium oxide. The crimpled steel fibres of length 30 mm and of diameter 0.50 mm were used in this study.

2.5 Super Plasticizer (SP): The high-range water-reducing superplasticizer based on a polycarboxylic ether formulation was employed in this work. The specific gravity of this superplasticizer was 1.08. When compared to conventional superplasticizers, this superplasticizer has a unique chemical structure. It is a polymer of long-chain carboxylic ethers. The identical electrostatic dispersal mechanism was started at the initial stage of hydration, but the adjacent chains attached to the polymer backbone created a steric barrier that regulated the ability of cement particles to split and disperse them through Reversible Addition-Fragmentation Chain Transfer (RAFT) polymerization as shown in Figure 1 [Yang, et.al, 2024]. This steric interference created a physical barrier between the cement grains. The flowable concrete with considerably less water content can be obtained through the use of this technique.

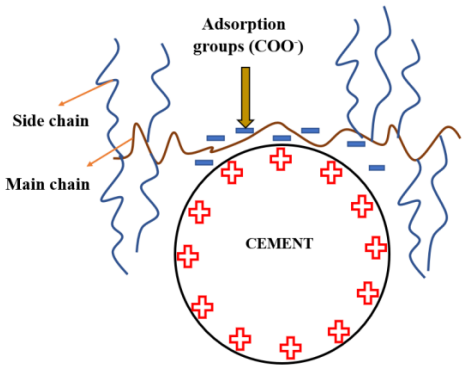

Figure 1. RAFT Polymerisation process

3. Experimental Programme

3.1 Mixing and casting

There is no codal provision for the mix proportion of RPC, so it was chosen based on several literatures [Rajasekar, et.al, 2019 and Lessly, et.al, 2020]. The attempt was taken to

reduce the cement content; first, three ratios, M1, M2, and M3, were explored as shown in Table 1, and cubes were cast based on them. The water-to-binder ratio (w/b) plays a vital role in the mix design of RPC. A higher w/b ratio leads to higher workability but reduces the strength, whereas a lower w/b ratio leads to higher strength and durability, but it significantly impacts workability. So, optimizing this w/b ratio is a crucial part of designing RPC with higher strength and workability. Another important parameter is the amount of superplasticizer, which determines the workability, strength, and durability. Typical dosages of superplasticizer vary from 0.5% to 3%. Lesser superplasticizer dosage reduces the workability and flowability of concrete, whereas higher superplasticizer dosage leads to bleeding, segregation, and delay in setting time. Here, a series of trial mixes were performed by varying the w/b ratio from 0.15 to 0.20 and the superplasticizer dosage from 1% to 2% by weight of cement. Based on the flowability results and visual stability, the w/b ratio was reduced from 0.17 for M1 to 0.15 for M4, whereas the superplasticizer dosage was increased from 1.5% in the control mix to 1.6% in M4 to have good workability, especially flowability, and high strength. The control mix was first optimized, after which 10 % of the cement was partially replaced with Alccofine, and 40 % of the quartz sand was substituted with copper slag in the fourth ratio, M4. These replacement levels were selected based on preliminary trial mixes with all ratios of alccofine and copper slag, previous literature, and to balance strength and sustainability objectives. The higher dosages of alcofine (more than 10%) are found to reduce both workability and strength, and copper slag dosages above 40% led to bleeding and segregation in trial mixes. These results were also proposed by Sagar & Sivakumar, (2020) who stated that, alccofine was incorporated at 10 % by weight of cement due to its high fineness and its ability to enhance early-age strength and densify the microstructure. Copper slag was used at 40 % by weight of quartz sand, as prior studies reported that a 40–50 % replacement improved density and reduced permeability due to dense particle packing, as evidenced by Pushpakumara & Bandara, (2025). Especially when replacing 40% for fine aggregate, it increased the workability and strength of concrete, reduced

water absorption coefficient and chloride permeability, and improved resistance to sulphate attack [Nieświec, et.al., 2025] In trial mixes, the cubes with the combination of 10% alccofine and 40% copper slag showed optimal performance by giving good workability and strength.

Table 1. Chosen Mix ratio of RPC

Constituents	M1	M2	M3	M4
Cement (kg m^{-3})	800	850	900	810
Silica Fume (kg m^{-3})	220	225	230	230
Quartz Sand (kg m^{-3})	800	825	850	510
Quartz Powder (kg m^{-3})	70	85	90	90
Steel Fibre (kg m^{-3})	119	119	119	119
Superplasticizer (%)	1.5	1.5	1.5	1.6
Water (ml)	170	170	168	168
Alccofine (kg m^{-3})	-	-	-	90
Copper Slag (kg m^{-3})	-	-	-	340
Water to binder ratio (W/b)	0.17	0.16	0.15	0.15

As shown in Figure 2, all the dry materials and steel fibres were mixed for 2 minutes at low speed (140 rpm), then half the amount of water and superplasticizer was added and mixed for 5 minutes at high speed (285 rpm), and finally the remaining water and superplasticizer were added and mixed for 3 minutes at the same high speed. After mixing, the mix was poured into the moulds and allowed to set for 1 day. Then the specimens were demoulded and placed in a curing chamber.

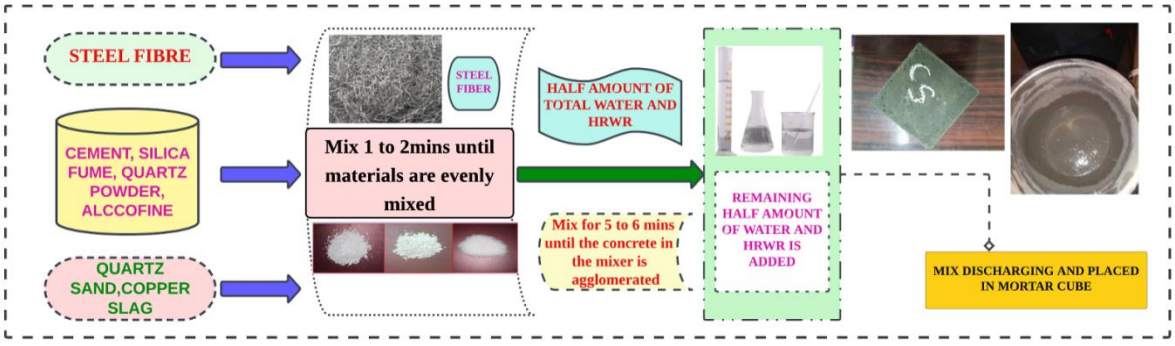

Figure 2. Mixing technique of RPC

3.2 Various curing techniques

Four types of curing were performed in this work, such as water curing, boil water curing, hot air curing, and autoclave curing. In water curing, the specimens after demoulding were submerged in water for 28 days to achieve the target strength as per IS 456:2000. In boil water curing, the specimens with the mould were cured for three hours by placing them inside the curing tank full of boiling water with a temperature of 100°C as per IS:9013-1978. In hot air curing, the specimens after demoulding were exposed to the hot air in hot air ovens at temperatures of 100 °C to 200 °C for 24 hours. Hot air temperatures that stay high for long periods of time could lead to the formation of secondary hydration components such as xonotlite and tobermorite. Secondary tobermorite structures were discovered after 3 days of curing at temperatures of 100 °C and 150 °C in hot air ovens, and xonotlite secondary substances were observed after 3 days of curing at temperatures of 150 °C and 200 °C in hot air ovens. In autoclave curing, the specimens after demoulding were placed in the horizontal autoclave with a pressure of 1.5 bar for 18 hours. During autoclaving, the high strength attained is mostly due to the result of the synthesis of tobermorite and xonotlite. For both hot air curing and autoclave curing, the duration and temperatures were chosen based on the previous literature [Rajasekar, et.al., 2019], and curing was carried out as per the procedure given in IS 6461-7 (1973). In hot air curing, this elevated temperature accelerated hydration and enhanced the strength of concrete. In autoclave curing, the duration was reduced and the pressure was increased to enhance strength and reduce porosity of RPC.

3.3 Strength and durability tests

After curing, various tests such as compressive strength, residual compressive strength after elevated temperature exposure, water absorption, sorptivity, rapid chloride penetration test, impact strength, and acid attack were performed on the specimens as described below. To ensure reliability and consistency of the results, three specimens were cast and tested for each mix

under all experimental and curing conditions. The average of the three test values is reported in Table 2.

3.3.1 Compressive strength:

The concrete cubes of size 70.6 mm were cast. After that, the curing of specimens was done under various curing conditions, such as water curing, boil water curing, autoclave curing, and oven curing. The compressive strength of specimens was evaluated after a considerable period of time that varies for every curing. Typically, force was applied through a hydraulic press at the top of the specimen until failure occurred. The load was applied at a steady rate of 0.60 MPa per second until the specimen failed as per IS 516:1959. The compressive strength was calculated by recording the highest load applied to the specimen and dividing that into its cross-sectional area.

3.3.2 Residual compressive strength under elevated temperature

The first stage in placing RPC through its test is to keep the concrete specimens ready for the elevated temperature. After curing, the specimens were placed in a furnace, and the heating was done at a temperature determined by the demands of the test. In this study, temperatures of 300 °C, 600 °C and 900 °C were employed. The effects of heating the specimens were monitored in real time by placing them in an oven at the above-mentioned temperatures. The purpose of this experiment is to learn how concrete reacts to extreme heat. These temperatures were chosen based on previous research by Aygörmez, et.al (2020) and Sevinc & Durgun (2023). They stated that after 300 °C, the decomposition of the tobermorite layer occurred, and evaporation of chemically bound water led to shrinkage and cracking, which was the starting of thermal damage. After 600 °C, the decomposition of carbonates occurred and weakened the concrete further, which was the trigger of irreversible damage. After 900 °C, the entire concrete was subjected to spalling and cracking, which led to damage of the entire structure.

3.3.3 Water Absorption

The strength of a concrete specimen and its weathering resistance could be evaluated by measuring the ability of the concrete to absorb water. After curing, the initial weight was noted by weighing all the specimens. The samples were stored in water in a sealed container to prevent loss due to evaporation and left to soak for 60 days. Then, the samples were taken out of the water and wiped off with a towel. The percentage of water absorption was found by taking the difference in weight before and after soaking and dividing it into the initial weight.

3.3.4 Water sorptivity

Sorptivity refers to a concrete's capacity to take in water by capillary action. The sorptivity was calculated using the procedures specified by ASTM C 1585. Concrete's strength and permeability were evaluated with this attribute. After curing, the initial weights of the cube specimens were recorded. The specimens were placed in the water reservoir having a water depth of 5 mm, with their bottom area in contact with water. The specimens were weighed again after soaking.

The sorptivity of the concrete is calculated from the weight, area of the specimen, density of water, and elapsed time, as expressed in equation (1).

$$S = \frac{m_2 - m_1}{Adt^{1/2}} \quad (1)$$

where S is the sorptivity, m_1 is the initial weight of the sample, m_2 is the final weight of the sample after soaking, A is the surface area of the specimen at the bottom, d is the density of water and $t^{1/2}$ is the elapsed time.

3.3.5 Rapid Chloride Penetration Test (RCPT)

Concrete's chloride incorporation is often evaluated using the RCPT. This test will be useful to determine the longevity of concrete structures in places like coastal areas, where chloride ions can infiltrate and induce corrosion of reinforcing steel. Two electrodes were attached to the opposite sides of the specimen. The sample was then subjected to 60 V DC for 6

hours. During this time, the supplied voltage drives the chloride ions through the concrete specimen. At regular intervals, the amount of current flowing through the specimen was observed as per ASTM C1202. The quantity of charge that has travelled through the specimen was measured after 6 hours. Lower RCPT (Rapid Chloride Permeability Test) scores are desirable as they indicate superior durability and a lengthier lifespan, especially in settings that are exposed to deicing salts or sea conditions, where the corrosion of reinforcement caused by chloride is a significant worry.

3.3.6 Impact strength

An impact test was used to evaluate the impact strength. The specimens were broken by dropping a disc of mass 4.60 kg from a height of 500 mm. The force was transmitted from the hammer to the top surface of the sample through a 65 mm ball that was positioned at the center of the disc. By using this procedure, the number of blows required to break the specimens (n) can be found, and the impact strength (kilo Joules) can be calculated using equation *(2)*.

$$\text{Impact Strength(kJ)} = \frac{n * m * g * h}{1000} \quad (2)$$

where, m-mass of disc 'kg'; g- acceleration due to gravity (m s^{-2}); h- the height of drop(m)

Greater impact strength signifies superior toughness and resilience against dynamic or impact pressures, making it crucial for applications like pavements, industrial floors, and structures exposed to heavy machinery or automobile traffic.

3.3.7 Acid attack

In order to determine the resistance of specimens to acid attack, cured specimens were immersed in hydrochloric acid (HCl) of pH 2 for 60 days. The loss in the mass of specimens after 60 days indicated the vulnerability of the concrete to acid.

3.3.8 Analysis of Variance (ANOVA)

ANOVA was performed to know whether the results were statistically significant between all the mix ratios (M1 to M4) and all the curing conditions. This statistical analysis was followed by the post-hoc Tukey HSD (Honest Significant Difference) test with the confidence level of 95 % (p=0.05).

3.3.9 Scanning Electron Microscopy (SEM)

SEM images are used to learn more about the distribution of particle sizes, morphology, and surface properties. The pictures are additionally useful for detecting any pollutants or impurities in the material. SEM images of silica fume, quartz powder, quartz sand, copper slag, alccofine, cement are shown in Figure 3. The SEM image of silica fume revealed the presence of very fine spherical particles of size 0.50 μm. This high fineness and smooth morphology promoted pozzolanic reactivity and improved particle packing, thereby reducing porosity and enhancing microstructural densification. The SEM image of quartz powder revealed several irregular angular particles with sharp edges of size less than 50 μm. The angular morphology of quartz powder enhanced mechanical interlocking within the cementitious matrix, thereby contributing to the development of ultra-high-strength concrete. The SEM image of quartz sand revealed large, irregular, angular particles with sharp edges and no agglomeration of size less than 1 mm. This coarse particle size contributed to the skeletal framework of the concrete matrix and enhanced dimensional stability. The SEM image of copper slag revealed the presence of irregular, sharp-edged angular particles of 2 mm with more voids. This angular particle improved mechanical interlocking within the cementitious matrix, and the glassy amorphous phase enhanced its latent pozzolanic reactivity. The SEM image of alccofine showed that it consists of ultrafine, irregular-shaped smooth surfaces with agglomeration having a size less than 1 μm. The minute particle enhanced its reactivity, contributed to the filler effect, promoted pozzolanic activity, and resulted in additional C–S–H gel formation, which enhanced strength development. The SEM image of cement revealed the presence of an irregular smooth texture

388 with no voids less than 100 µm. This heterogeneous surface texture enhanced water adsorption
389 and initiated hydration reactions.

390 **3.3.10 Energy-Dispersive X-ray analysis (EDAX)**

391 Energy-dispersive x-ray analysis (EDAX) is an effective method for analyzing materials
392 down to the atomic level. It is widely employed in the investigation of materials, especially silica
393 fume, in the fields of materials and engineering. EDAX refers to the X-rays produced when an
394 object is exposed to an electron beam. The elements contained in the sample determine the
395 properties and nature of the X-rays produced. Graphical results of EDAX of alccofine, quartz
396 powder, copper slag, and silica fume are shown in Figure 4. The EDAX images of silica fume
397 and quartz powder showed that it contains a high concentration of silicon and oxygen with trace
398 amounts of carbon, aluminum, iron, and magnesium. This confirms the composition as
399 amorphous silicon dioxide (SiO_2) in silica fume and crystalline silicon dioxide (SiO_2) in quartz
400 powder. Consequently, silica fume enhanced pozzolanic activity by forming additional C–S–H
401 gel, whereas quartz powder primarily acted as a filler material in concrete. The EDAX image of
402 copper slag revealed that it contains iron, silicon, and aluminum. The presence of these oxides
403 contributed to moderate pozzolanic activity. The EDAX image of alccofine revealed that it
404 contains high amounts of calcium, silicon, and aluminium with trace amounts of magnesium and
405 iron. It confirmed the composition as calcium silicate–aluminate material, which is responsible
406 for high reactivity.

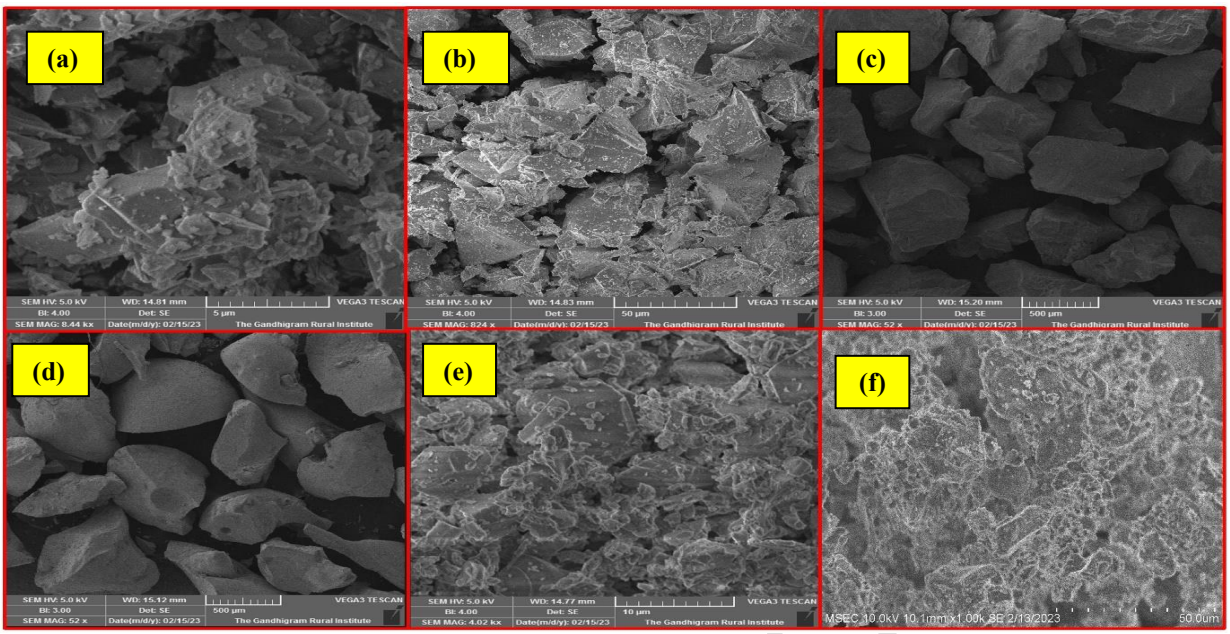

Figure 3. SEM Images of (a) Silica Fume (b) Quartz Powder (c) Quartz Sand (d) Copper Slag (e) Alccofine (f) Cement

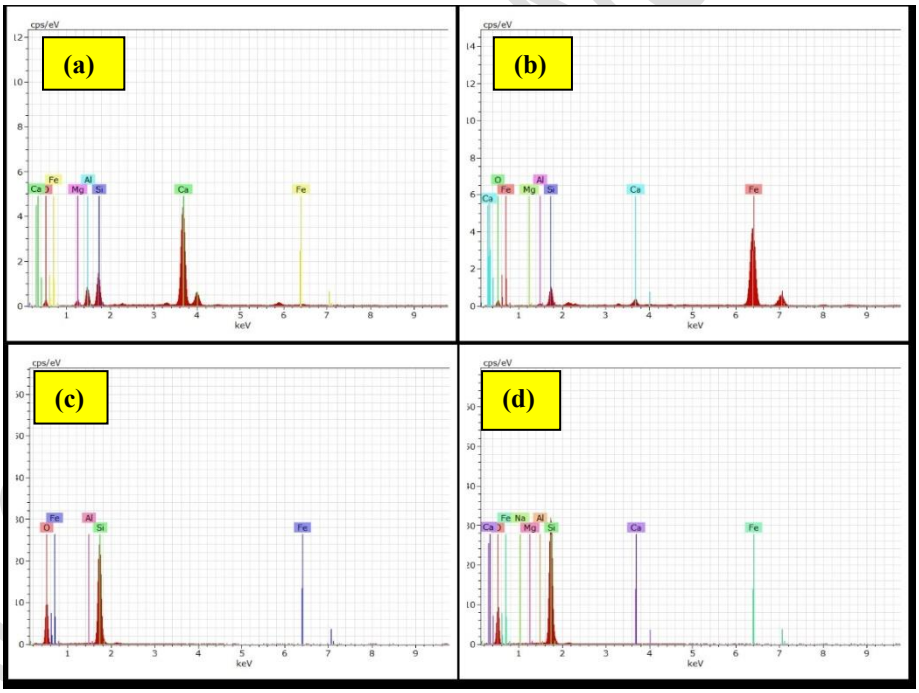

Figure 4. EDAX Images of (a) Silica Fume (b) Quartz Powder (c) Copper Slag (d) Alccofine

Figure 5 gives the overview of this work. In this overview, the materials for preparing RPC, tested properties and curing techniques followed in this work was shown.

414

415 *Figure 5. Project Overview*

416

4. Results and Discussion

The results of all the properties for all the ratios M1, M2, M3, and M4 are shown in Table 2 with their Standard Deviation (SD) and Standard Error (SE) to show the variability among the replicates and to emphasize the precision of the mean.

Table 2. Test results of RPC

S.No	Properties	M1			M2			M3			M4		
		Mean	SD	SE	Mean	SD	SE	Mean	SD	SE	Mean	SD	SE
1	**Compressive strength (MPa)**												
	a) Normal water curing	86.8	2.12	1.22	89.1	0.72	0.42	92.2	1.92	1.11	99.4	0.70	0.40
	b) Boil water curing	88.3	0.70	0.40	91.4	0.62	0.36	95.8	1.66	0.96	109.2	0.46	0.26
	c) Hot air curing	115.3	0.98	0.57	123.1	2.01	1.16	137.2	0.66	0.38	159.3	0.81	0.47
	d) Autoclave curing	125.9	1.21	0.70	136.2	1.06	0.61	149.8	2.79	1.61	176.5	0.62	0.36
2	**Residual compressive strength after elevated temperature (MPa)**												
	a) At 300° C	123.2	1.31	0.75	130.8	1.61	0.93	148.2	2.01	1.16	177.5	2.16	1.25
	b) At 600° C	91.6	1.45	0.84	102.7	2.35	1.36	111.9	1.05	0.61	128.9	1.35	0.78
	c) At 900° C	58.2	0.36	0.21	68.5	1.18	0.68	68.3	0.62	0.36	76.6	0.70	0.40
3	**Water sorptivity (mm/min$^{0.5}$)**	3.20	0.26	0.15	2.99	0.35	0.20	2.98	0.12	0.07	2.95	0.04	0.02
4	**Water Absorption (%)**	3.5	0.36	0.21	3.2	0.46	0.26	2.9	0.85	0.49	2.7	0.26	0.15
5	**RCPT**	42	1.73	1.00	43	1.73	1.00	38	1.00	0.58	29	1.73	1.00
6	**Impact Strength (kJ)**	2.56	0.05	0.03	2.48	0.08	0.05	2.77	0.06	0.03	2.80	0.05	0.03
7	**Acid attack (%)**	3.8	0.06	0.04	3.2	0.15	0.09	2.3	0.09	0.05	2.2	0.13	0.07

4.1 Compressive strength:

The compressive strengths of the specimens under various curing conditions are summarized quantitatively in Figure 6. The results showed that, from normal water curing, compressive strength increases to boil water curing, hot air curing, and autoclave curing for each mix ratio (M1, M2, M3, M4), and M4 achieved the highest strength in all curing conditions, maximum being 176.5±0.62 MPa. It indicated that more intense curing methods, particularly autoclave curing, more significant enhancement were achieved in concrete strength, especially for higher mix ratios. The autoclaving technique has significantly altered the microstructure of RPC. SEM image and mercury porosimetry findings validated these findings [Rong , et.al., 2020

and Sebastin, et.al., 2020]. Their study revealed that autoclave curing produced a denser microstructure with minimal porosity and additional crystalline phases like tobermorite, significantly enhancing the compressive strength. Normal water curing resulted in higher porosity and slow hydration, yielding lower strength. Boil water and hot air curing improved hydration and reduced porosity but are less effective than autoclave curing. Table 2 indicated that the crushing strength of the M4 mix specimen with autoclave curing is 176.5±0.62 MPa, which is higher, compared to all other specimens due to supplementary cementitious materials and also the incorporation of micro-steel fibre that arrested the shrinkage cracks in the specimen during heat treatment. Due to the low cement content in M1, it did not attain an enormous amount of strength (125.9±1.21 MPa, a 16 % decrease) compared to M3. But the difference in results between M1, M2, and M3 is not statistically significant. The compressive strength of the M4 specimen with alccofine and copper slag is 176.5±0.62 MPa, which is 17.82 % greater than the M3 specimen, which has 149.8±2.79 MPa. The difference in results between M3 and M4 is statistically significant, as evidenced by ANOVA analysis.

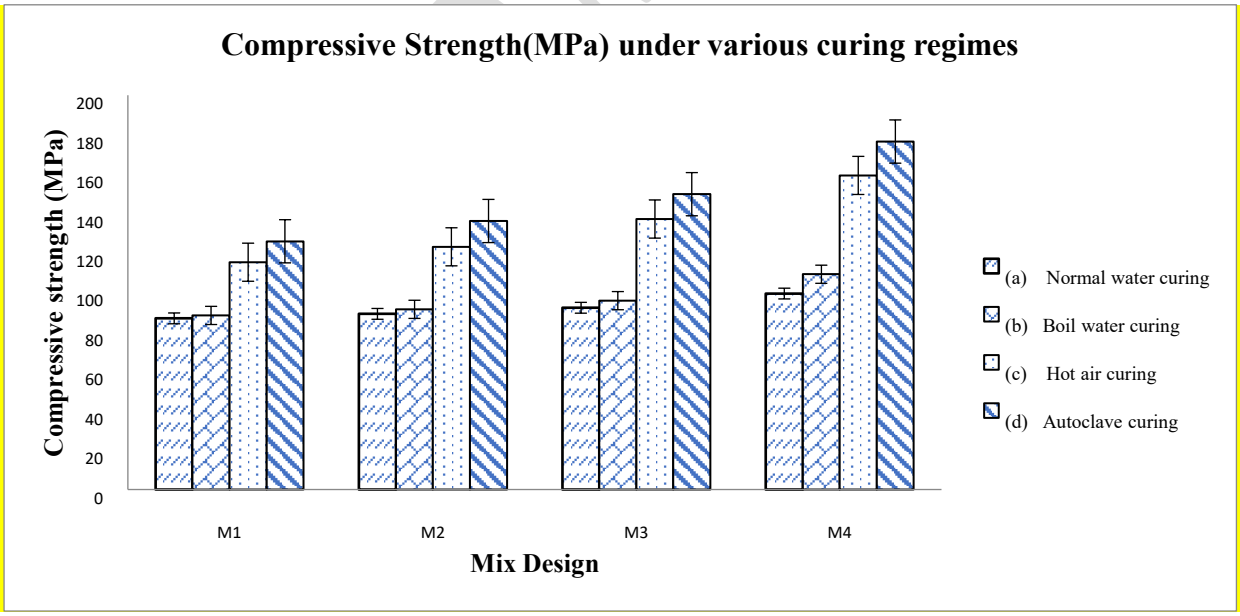

Figure 6. Compressive strength of RPC mixes under various curing conditions

4.2 Residual compressive strength under elevated temperature exposure

Any damages caused by the fire, such as cracking or spalling, were determined by visual examination. Their compressive strengths after elevated temperature exposure are shown in Table 2 and Figure 7. Cracking and spalling at the edges were observed in the specimens subjected to a temperature of 900°C. The compressive strengths of specimens of different mix ratios decreased with the increase in temperature, as shown in Figure 7. M4 specimens still had the maximum compressive strength of 177.5±2.16 MPa when exposed to different temperatures, which indicated that alccofine and copper slag have the capacity to resist the fire more than the cement and quartz sand. At a temperature of 300 °C, all mixtures maintained reasonably high levels of strength as 123.2±1.31 MPa, 130.8±1.61 MPa, 148.2±2.01 MPa and 177.5±2.16 MPa. However, significant deterioration was noticed at 600 °C, and even more so at 900 °C. It demonstrated the serious negative effect that high temperatures have on the integrity of concrete. The exceptional performance of mix M4 indicated that it is more suitable for applications that demand high thermal resilience. Under elevated temperature exposure of autoclave-cured specimens, M4 exhibited the highest strength of 177.5±2.16 MPa, 128.9±1.35 MPa, and 76.6±0.70 MPa at 300 °C, 600 °C and 900°C, respectively, compared to all other specimens. The compressive strength of M4 at 300°C was 177.5±2.16 MPa, which is 19.77 % greater than M3, having 148.2±2.01 MPa. The residual compressive strength of M4 under elevated temperature exposure at 900 °C was 56.85 % less than that at 300 °C.

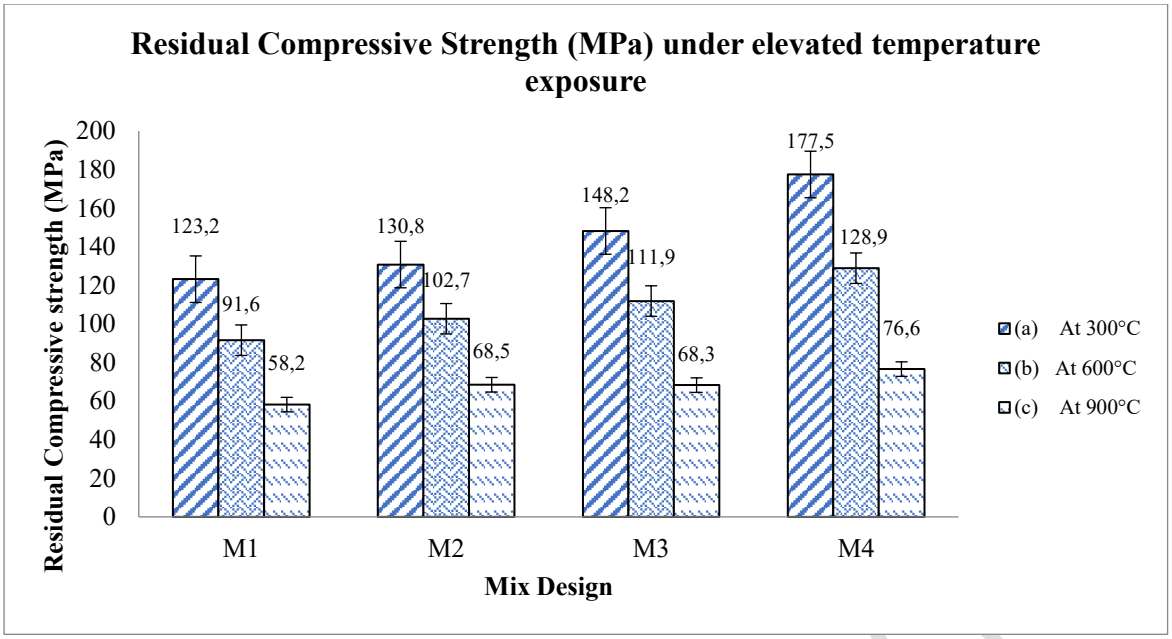

Figure 7. Residual compressive strength of different RPC mixes after exposure to elevated temperature

4.3 Water sorptivity

The test results indicated that M3 had a lower sorptivity value of 2.98 mm/min^{0.5} than all of M1 and M2 due to its high cementitious content. Table 2 and Figure 8 depicted the water sorptivity of four distinct concrete mixtures (M1, M2, M3, and M4), which quantifies the speed at which water is soaked up through capillary action. The findings indicated that M1 has the highest sorptivity, measured at a rate of 3.20±0.26 mm/min^{0.5}. The sorptivity values for M2 and M3 are slightly lower, measuring at 2.99±0.35 and 2.98±0.12 mm/min^{0.5}, respectively. These data indicated that M1 is more prone to water infiltration through capillary action in comparison to M2 and M3. M4 is having the lowest sorptivity of 2.95±0.04 mm/min^{0.5} which is 1% less than M3. A lower sorptivity level implies a higher resistance to water infiltration, which is essential for the long-term durability of concrete, particularly in situations with high moisture exposure.

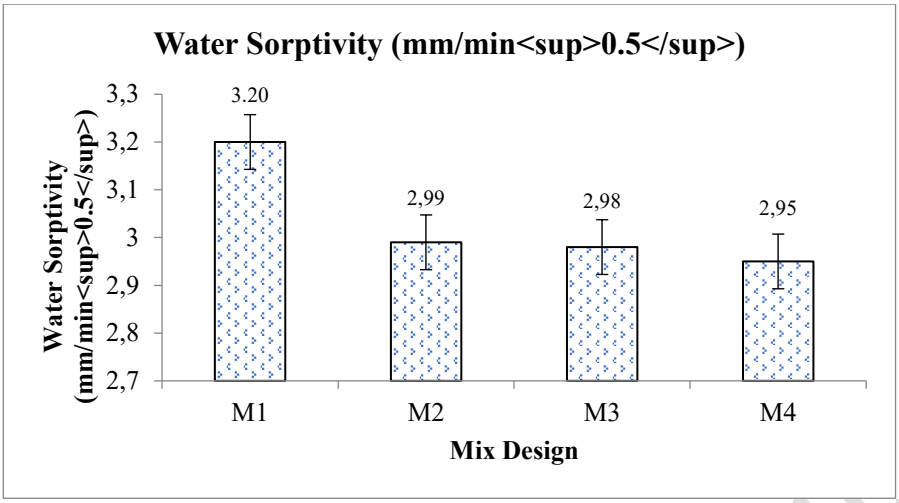

Figure 8. Water Sorptivity of different RPC mixes

4.4 Water Absorption

Table 2 and Figure 9 show the results of the water absorption test for the four concrete mix ratios. Water absorption is a quantitative assessment of the porosity of concrete and its capacity to suck up in water. M1 exhibited the greatest water absorption rate of 3.5±0.36 %, representing the highest level of porosity and potentially reduced durability. M2 had a water absorption rate of 3.2±0.46 %, followed by M3 at 2.9±0.85 %, and finally M4 with the lowest water absorption rate of 2.7±0.26 % which is 6.7% less than M3. The results suggested that M4 possessed the most compact microstructure, which is associated with its exceptional compressive strength and reduced permeability. Less water absorption is advantageous since it improves the concrete's durability against weathering, chemical corrosion, and freeze-thaw cycles. The results indicated that the addition of copper slag and alccofine created a dense packing concrete. It is inferred from the SEM image that copper slag and quartz sand have large pores that are filled with quartz powder, cement, and adding supplementary cementitious materials such as alccofine and silica fume to enhance RPC. Since both water sorptivity and water absorption depend on the packing of RPC, M3 and M4 cubes had the lowest water sorptivity and water absorption.

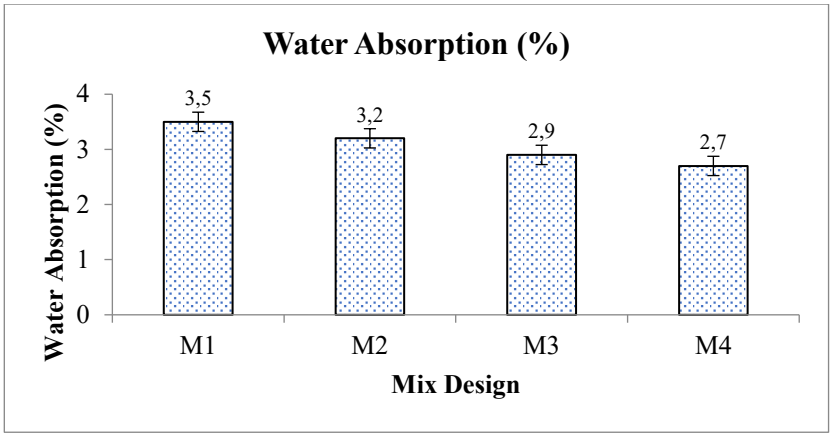

Figure 9. Water Absorption of different RPC mixes

4.5 Rapid Chloride Penetration Test (RCPT)

The quantity of charge passing through the specimens, in the range of 29-43 coulombs, indicates lower porous and impermeable characteristics. Table 2 and Figure 10 show the results from the Rapid Chloride Penetration Test (RCPT), where M1 and M2 had the most significant RCPT values, measuring 42±1.73 and 43±1.73 coulombs, respectively. It suggested that they possessed the greatest permeability and the least resistance to the penetration of chloride. The RCPT value of the M4 specimen was 29±1.73 coulombs, which is 31 % less than that of the M3 specimen, which had 38±1.00 coulombs, which indicated that the M4 specimen has less chloride ion penetration, and so the M4 RPC specimen is suitable for chloride content environments, as in offshore structures.

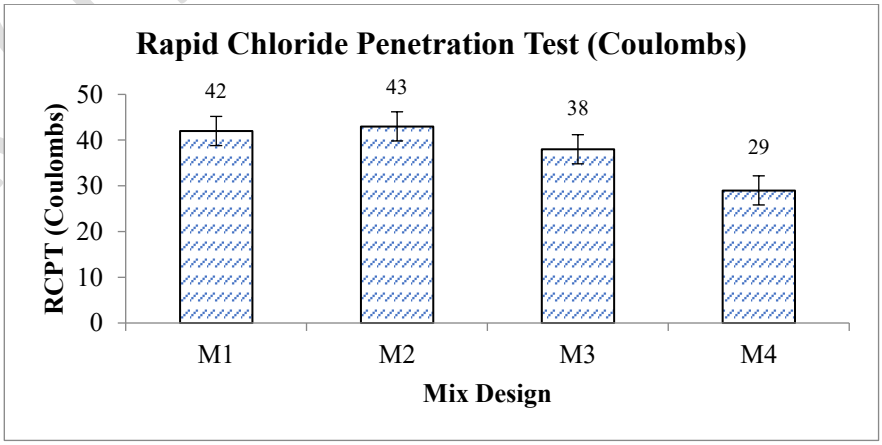

Figure 10. Rapid Chloride Penetration of different RPC mixes

4.6 Impact strength

Table 2 and Figure 11 display the impact strength of the specimens made with different mix ratios, where M4 exhibited superior capability in withstanding impact loads because of the addition of copper slag, which is one of the toughest materials, with M3 closely trailing behind. The impact strength of the M4 specimen was 2.80±0.05 kJ, which is higher than that of the M3 specimen by 1.07 % (2.77±0.06 kJ). The highest impact strength of the M4 specimen represented the addition of copper slag, which improved the toughness and durability of the specimen.

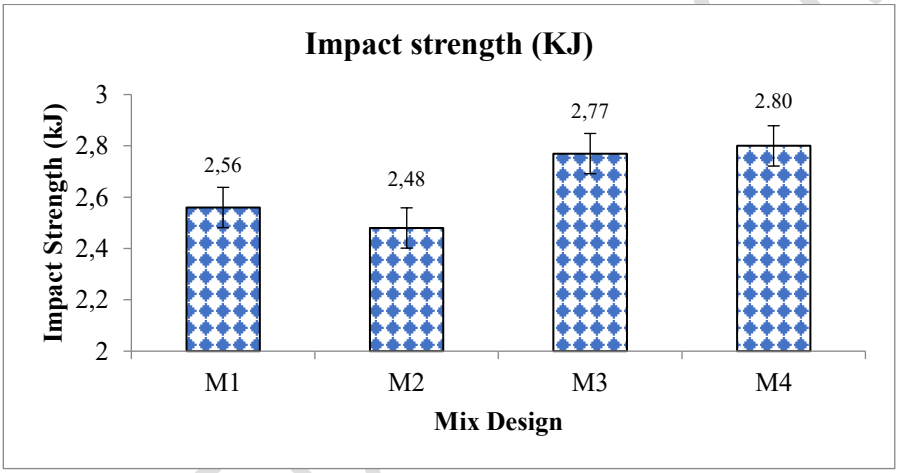

Figure 11. Impact Strength of different RPC mixes

4.7 Acid attack

In order to determine the resistance of specimens to acid attack, a test was carried out on RPC cube specimens. The greater resistance of RPC specimens to acid attack and the subsequent reduced weight loss with respect to mortar cube specimens indicated the decrease in permeability and the increase in durability. Table 2 and Figure 12 showed the reduction in the mass of specimens due to submergence in acid. Due to their lower permeability, M4 specimens exhibited the least mass reduction of 2.3 %, while M3 specimens showed a similar result of 2.2 %.

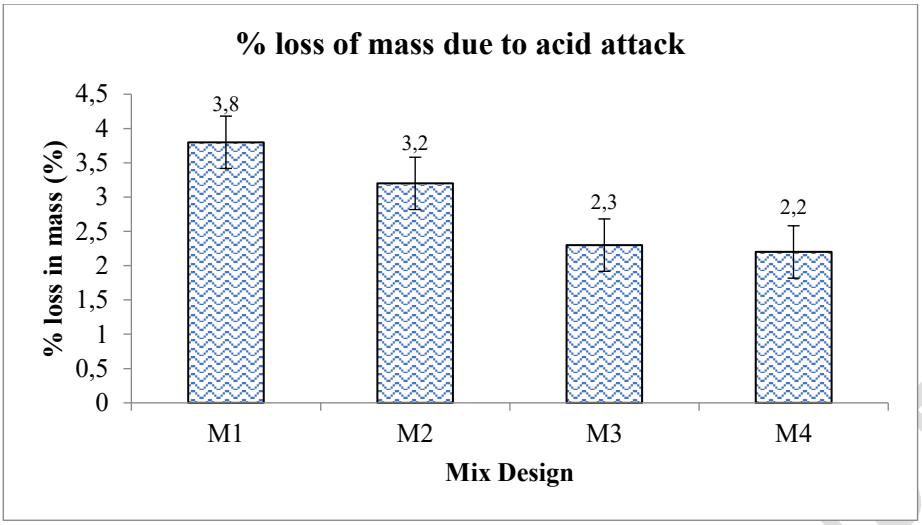

Figure 12. Mass loss of different RPC mixes after acid immersion

4.8 Comparison of results

The strength and durability performance of the proposed RPC mix (M4), which is sustainable, was compared with conventional cement concrete and other sustainable concrete reported in the literature. The results of testing with the proposed mix (M4) showed compressive strength and impact strength of 176.5 MPa and 2.8 MPa under autoclave curing, which is significantly higher than conventional cement concretes (20-70 MPa) and sustainable mixes containing waste fly ash, perlite powders, waste glass, and waste ceramic tiles with compressive strength in the range of 80 MPa to 105 MPa as reported by Abed & Nemes, (2019), and Radhi, et.al., (2021). The water absorption of the proposed mix (M4) showed results of 2.7 %, which is significantly lower than conventional cement concretes (4-6 %) and at par with sustainable concrete mixes with fly ash and GGBS having sorptivity of absorption about 2.5-3.5 % as reported by Siddique (2014). The rapid chloride penetration of the proposed mix (M4) was measured at 29 coulombs, which is significantly lower than the values for conventional concrete mixes (1000–4500 coulombs) and copper slag-incorporated ultra-high-strength concrete, which have RCPT values ranging from 100 to 150 coulombs. As per ASTM C1202, RCPT values with less than 100 coulombs have excellent resistance, which represents the proposed mix conforming to the code. The percentage loss of mass due to immersion in acid of the proposed

mix M4 was 2.2 % which is significantly lower than conventional concrete mixes (2-5 %) and sustainable concrete mixes with waste granite sand having a value range between 2 and 4 % [Rajasekar, et.al., 2018a]. Here, the durability tests, such as water absorption and acid resistance, were tested after 60 days, while compressive strength was measured after 28 days. The improved performance was observed after 60 days of durability tests due to the presence of silica fume and alccofine, which improved the hydration and pozzolonic reaction. These materials contributed to ongoing densification of microstructure and additional formation of CSH gel, thereby reducing porosity and improving resistance to water absorption and loss of mass due to immersion in acid. The aging effect was pronounced in mixes including silica fume and alccofine, where long-term curing enhanced durability of RPC because of reduced permeability and continued pozzolonic activity.

4.9 Analysis of Variance

A two-way analysis of variance (ANOVA) was conducted to assess the influence of curing conditions and mix design on the compressive strength of RPC. This study considered two independent variables such as curing method (normal water curing, boil water curing, hot air curing & autoclave curing) and mix ratio (M1, M2, M3 & M4) as levels and one dependent variable as compressive strength.

Table 3. ANOVA Summary

	sum_sq	df	F	PR(>F)
C(Mix)	9491.7843	3.0	2245.300729	1.386927e-51
C(Curing)	36480.8043	3.0	8629.607868	1.461014e-65
C(Mix):C(Curing)	2192.1289	9.0	172.850838	1.918976e-33
Residual	67.6384	48.0	NaN	NaN

The ANOVA results revealed that high correlation occurred for the effects and interaction between various mixes and curing conditions. Especially, the curing conditions had a high influence on compressive strength, as evidenced from Table 3, which shows an F-statistic of 8629.607868 ($p<0.0001$). Similarly, the mix ratio had a significant contribution to compressive strength, as the F-statistic indicated by a value of 2245.300729 ($p<0.0001$). The

highly significant interaction occurred between the mix ratio and the curing condition, where the F statistic is 172.850838 ($p<0.0001$). The results inferred that depending on the mix design, the response to the curing condition changes. The compressive strength of RPC was not only independently influenced by mix design and curing conditions but also by specific combinations of these factors, like the mixes with high cement and pozzolonic content that achieved ultra-high strength under autoclave curing, whereas less intensive curing methods were associated with relatively lower strengths across most mixes. This enlightens the need for a tailored approach while selecting curing conditions of RPC with different formulations.

Among the curing techniques evaluated, autoclave curing proved to be the best to have high compressive strength, where this curing promoted accelerated hydration and formation of denser microstructures. Hot air curing also resulted in substantial strength improvements compared to water-based methods, though to a lesser extent than autoclave treatment. Boil water and normal water curing yielded comparatively lower compressive strengths, which limited the effectiveness in developing ultra-high-strength RPC.

Among the mix ratios evaluated, the mixes that have greater amounts of cement, silica fume, and supplementary additives performed better in compressive strength, where they promote particle packing theory and refinement of pore structure. However, the interaction showed that even high-performance mixes require appropriate curing conditions to realize their optimal strength.

This model explained the vast majority of the variability in the data, reflected by the exceptionally large sums of squares attributed to the main effects and their interaction, compared to the relatively small residual error variance. These findings enlightened the importance of both the curing environment and the mix proportions in determining the compressive strength of concrete. The residual diagnostics analyses confirmed that model assumptions were adequately satisfied: residuals were approximately normally distributed and displayed no discernible patterns in the residuals-versus-fitted plot as shown in Figure 13, suggesting homogeneity of

variance across treatment combinations. While minor deviations were observed in the extreme quantiles of the Q-Q plot shown in Figure 13, these were not severe enough to compromise the validity of the analysis. The relatively low residual error variance further highlights the reliability of model estimates. It is important to note that this study employed three replicates per combination; in field applications, the practical viability will be lower due to several factors such as differences in mixing, compaction, and environmental exposure.

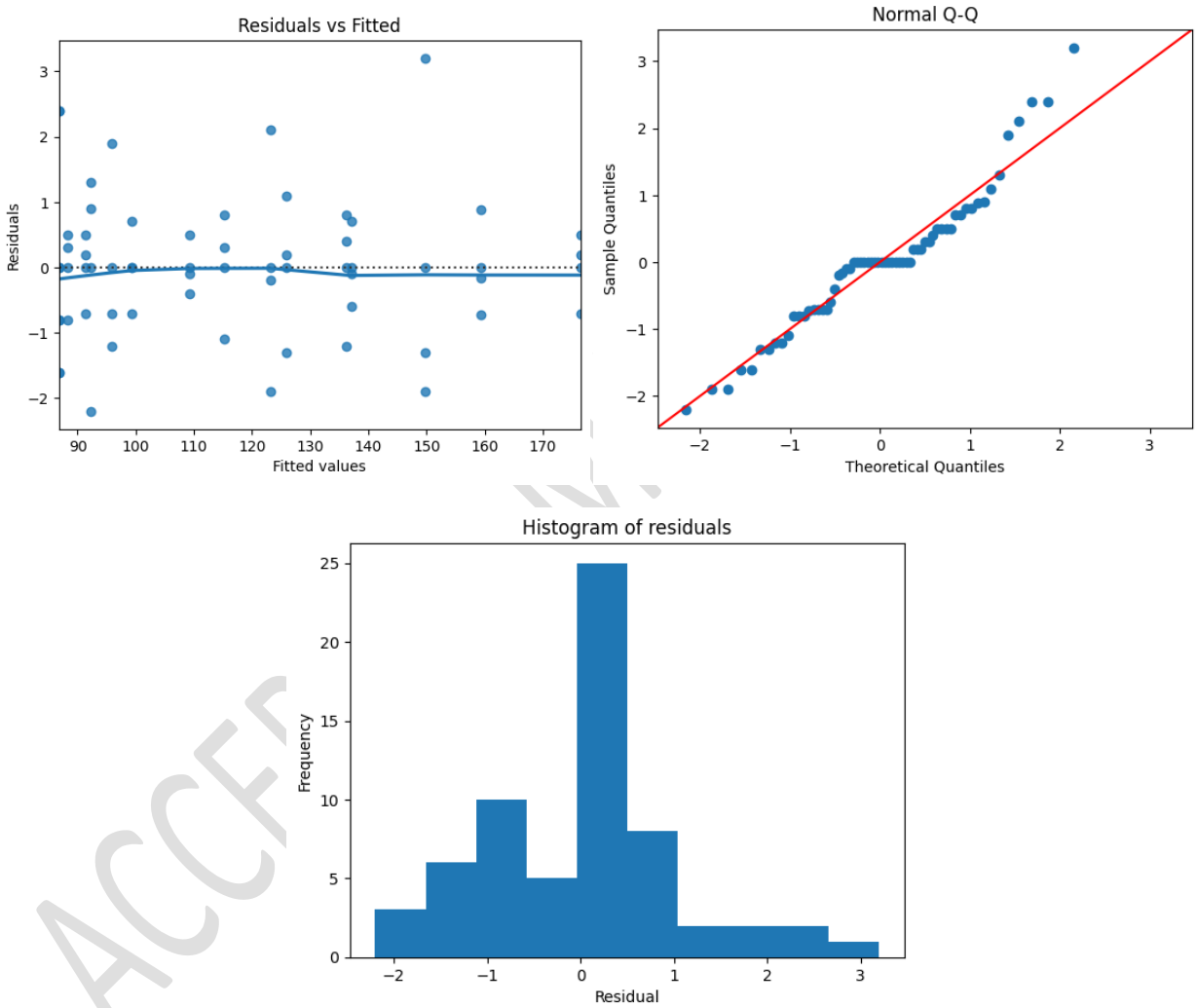

Figure 13. Diagnostic plots of two way ANOVA

4.9.1 Tukey's Honest Significant Difference (HSD) Test

In continuation with ANOVA, Tukey's HSD test were conducted to find which specific pairs of curing methods and mix ratios and their combinations differed significantly in compressive strength.

Tukey HSD - Curing Method:

Multiple Comparison of Means - Tukey HSD, FWER=0.05

Table 4. Pairwise Comparison among curing methods

group1	group2	meandiff	p-adj	lower	upper	reject
Autoclave curing	Boil water curing	-50.925	0.0	-64.0001	-37.8499	True
Autoclave curing	Hot air curing	-13.37	0.0432	-26.4451	-0.2949	True
Autoclave curing	Normal Water	-55.8	0.0	-68.8751	-42.7249	True
Boil water curing	Hot air curing	37.555	0.0	24.4799	50.6301	True
Boil water curing	Normal Water	-4.875	0.7584	-17.9501	8.2001	False
Hot air curing	Normal Water	-42.43	0.0	-55.5051	-29.3549	True

The pairwise comparison study among curing methods shown in Table 4 revealed that autoclave curing achieved the highest compressive strength compared to all mixes. Especially, the autoclave curing outperformed normal water and boil water curing with mean differences exceeding 50 MPa ($p < 0.001$) and also surpassed hot air curing by an average of approximately 13 MPa ($p = 0.043$). Hot air curing was significantly superior to both boil water and normal water curing, while boil water curing and normal water curing did not differ significantly from each other ($p = 0.758$). These findings highlighted the benefit of applying elevated temperature and pressure during curing.

Table 5. Pairwise Comparison among mix ratios

group1	group2	meandiff	p-adj	lower	upper	reject
M1	M2	5.3	0.9347	-18.44	29.04	False
M1	M3	14.675	0.368	-9.065	38.415	False

M1	M4	32.03	0.0039	8.29	55.77	True
M2	M3	9.375	0.7247	-14.365	33.115	False
M2	M4	26.73	0.0213	2.99	50.47	True
M3	M4	17.355	0.2259	-6.385	41.095	False

The pairwise comparison among mix ratios, which is shown in Table 5, revealed that the most enriched mix (M4) produced compressive strength significantly higher than M1 (mean difference ~32 MPa, p = 0.0039) and M2 (mean difference ~27 MPa, p = 0.0213). However, no significant differences were observed among the other pairwise comparisons, proving that the remarkable strength enhancement is mainly attributed to the high level of cement and pozzolonic material replacement.

Table 6. Pairwise Comparison among interaction

group1	group2	meandiff	p-adj	lower	upper	reject
M1-Autoclave curing	M1-Boil water curing	-37.6	0.0	-40.6324	-34.5676	True
M1-Autoclave curing	M1-Hot air curing	-10.6	0.0	-13.6324	-7.5676	True
M1-Autoclave curing	M1-Normal Water	-39.1	0.0	-42.1324	-36.0676	True
M1-Autoclave curing	M2-Autoclave curing	10.3	0.0	7.2676	13.3324	True
M1-Autoclave curing	M2-Boil water curing	-34.5	0.0	-37.5324	-31.4676	True
M1-Autoclave curing	M2-Hot air curing	-2.8	0.0993	-5.8324	0.2324	False
M1-Autoclave curing	M2-Normal Water	-39.1	0.0	-42.1324	-36.0676	True
M1-Autoclave curing	M3-Autoclave curing	23.9	0.0	20.8676	26.9324	True
M1-Autoclave curing	M3-Boil water curing	-30.1	0.0	-33.1324	-27.0676	True
M1-Autoclave curing	M3-Hot air curing	11.3	0.0	8.2676	14.3324	True
M1-Autoclave curing	M3-Normal Water	-33.7	0.0	-36.7324	-30.6676	True
M1-Autoclave curing	M4-Autoclave curing	50.6	0.0	47.5676	53.6324	True
M1-Autoclave curing	M4-Boil water curing	-16.7	0.0	-19.7324	-13.6676	True
M1-Autoclave curing	M4-Hot air curing	33.42	0.0	30.3876	36.4524	True
M1-Autoclave curing	M4-Normal Water	-26.5	0.0	-29.5324	-23.4676	True
M1-Boil water curing	M1-Hot air curing	27.0	0.0	23.9676	30.0324	True
M1-Boil water curing	M1-Normal Water	-1.5	0.909	-4.5324	1.5324	False
M1-Boil water curing	M2-Autoclave curing	47.9	0.0	44.8676	50.9324	True
M1-Boil water curing	M2-Boil water curing	3.1	0.0405	0.0676	6.1324	True

M1-Boil water curing	M2-Hot air curing	34.8	0.0	31.7676	37.8324	True
M1-Boil water curing	M2-Normal Water	-1.5	0.909	-4.5324	1.5324	False
M1-Boil water curing	M3-Autoclave curing	61.5	0.0	58.4676	64.5324	True
M1-Boil water curing	M3-Boil water curing	7.5	0.0	4.4676	10.5324	True
M1-Boil water curing	M3-Hot air curing	48.9	0.0	45.8676	51.9324	True
M1-Boil water curing	M3-Normal Water	3.9	0.0025	0.8676	6.9324	True
M1-Boil water curing	M4-Autoclave curing	88.2	0.0	85.1676	91.2324	True
M1-Boil water curing	M4-Boil water curing	20.9	0.0	17.8676	23.9324	True
M1-Boil water curing	M4-Hot air curing	71.02	0.0	67.9876	74.0524	True
M1-Boil water curing	M4-Normal Water	11.1	0.0	8.0676	14.1324	True
M1-Hot air curing	M1-Normal Water	-28.5	0.0	-31.5324	-25.4676	True
M1-Hot air curing	M2-Autoclave curing	20.9	0.0	17.8676	23.9324	True
M1-Hot air curing	M2-Boil water curing	-23.9	0.0	-26.9324	-20.8676	True
M1-Hot air curing	M2-Hot air curing	7.8	0.0	4.7676	10.8324	True
M1-Hot air curing	M2-Normal Water	-28.5	0.0	-31.5324	-25.4676	True
M1-Hot air curing	M3-Autoclave curing	34.5	0.0	31.4676	37.5324	True
M1-Hot air curing	M3-Boil water curing	-19.5	0.0	-22.5324	-16.4676	True
M1-Hot air curing	M3-Hot air curing	21.9	0.0	18.8676	24.9324	True
M1-Hot air curing	M3-Normal Water	-23.1	0.0	-26.1324	-20.0676	True
M1-Hot air curing	M4-Autoclave curing	61.2	0.0	58.1676	64.2324	True
M1-Hot air curing	M4-Boil water curing	-6.1	0.0	-9.1324	-3.0676	True
M1-Hot air curing	M4-Hot air curing	44.02	0.0	40.9876	47.0524	True
M1-Hot air curing	M4-Normal Water	-15.9	0.0	-18.9324	-12.8676	True
M1-Normal Water	M2-Autoclave curing	49.4	0.0	46.3676	52.4324	True
M1-Normal Water	M2-Boil water curing	4.6	0.0002	1.5676	7.6324	True
M1-Normal Water	M2-Hot air curing	36.3	0.0	33.2676	39.3324	True
M1-Normal Water	M2-Normal Water	0.0	1.0	-3.0324	3.0324	False
M1-Normal Water	M3-Autoclave curing	63.0	0.0	59.9676	66.0324	True
M1-Normal Water	M3-Boil water curing	9.0	0.0	5.9676	12.0324	True
M1-Normal Water	M3-Hot air curing	50.4	0.0	47.3676	53.4324	True
M1-Normal Water	M3-Normal Water	5.4	0.0	2.3676	8.4324	True
M1-Normal Water	M4-Autoclave curing	89.7	0.0	86.6676	92.7324	True
M1-Normal Water	M4-Boil water curing	22.4	0.0	19.3676	25.4324	True
M1-Normal Water	M4-Hot air curing	72.52	0.0	69.4876	75.5524	True
M1-Normal Water	M4-Normal Water	12.6	0.0	9.5676	15.6324	True
M2-Autoclave curing	M2-Boil water curing	-44.8	0.0	-47.8324	-41.7676	True
M2-Autoclave curing	M2-Hot air curing	-13.1	0.0	-16.1324	-10.0676	True
M2-Autoclave curing	M2-Normal Water	-49.4	0.0	-52.4324	-46.3676	True

M2-Autoclave curing	M3-Autoclave curing	13.6	0.0	10.5676	16.6324	True
M2-Autoclave curing	M3-Boil water curing	-40.4	0.0	-43.4324	-37.3676	True
M2-Autoclave curing	M3-Hot air curing	1.0	0.9976	-2.0324	4.0324	False
M2-Autoclave curing	M3-Normal Water	-44.0	0.0	-47.0324	-40.9676	True
M2-Autoclave curing	M4-Autoclave curing	40.3	0.0	37.2676	43.3324	True
M2-Autoclave curing	M4-Boil water curing	-27.0	0.0	-30.0324	-23.9676	True
M2-Autoclave curing	M4-Hot air curing	23.12	0.0	20.0876	26.1524	True
M2-Autoclave curing	M4-Normal Water	-36.8	0.0	-39.8324	-33.7676	True
M2-Boil water curing	M2-Hot air curing	31.7	0.0	28.6676	34.7324	True
M2-Boil water curing	M2-Normal Water	-4.6	0.0002	-7.6324	-1.5676	True
M2-Boil water curing	M3-Autoclave curing	58.4	0.0	55.3676	61.4324	True
M2-Boil water curing	M3-Boil water curing	4.4	0.0004	1.3676	7.4324	True
M2-Boil water curing	M3-Hot air curing	45.8	0.0	42.7676	48.8324	True
M2-Boil water curing	M3-Normal Water	0.8	0.9998	-2.2324	3.8324	False
M2-Boil water curing	M4-Autoclave curing	85.1	0.0	82.0676	88.1324	True
M2-Boil water curing	M4-Boil water curing	17.8	0.0	14.7676	20.8324	True
M2-Boil water curing	M4-Hot air curing	67.92	0.0	64.8876	70.9524	True
M2-Boil water curing	M4-Normal Water	8.0	0.0	4.9676	11.0324	True
M2-Hot air curing	M2-Normal Water	-36.3	0.0	-39.3324	-33.2676	True
M2-Hot air curing	M3-Autoclave curing	26.7	0.0	23.6676	29.7324	True
M2-Hot air curing	M3-Boil water curing	-27.3	0.0	-30.3324	-24.2676	True
M2-Hot air curing	M3-Hot air curing	14.1	0.0	11.0676	17.1324	True
M2-Hot air curing	M3-Normal Water	-30.9	0.0	-33.9324	-27.8676	True
M2-Hot air curing	M4-Autoclave curing	53.4	0.0	50.3676	56.4324	True
M2-Hot air curing	M4-Boil water curing	-13.9	0.0	-16.9324	-10.8676	True
M2-Hot air curing	M4-Hot air curing	36.22	0.0	33.1876	39.2524	True
M2-Hot air curing	M4-Normal Water	-23.7	0.0	-26.7324	-20.6676	True
M2-Normal Water	M3-Autoclave curing	63.0	0.0	59.9676	66.0324	True
M2-Normal Water	M3-Boil water curing	9.0	0.0	5.9676	12.0324	True
M2-Normal Water	M3-Hot air curing	50.4	0.0	47.3676	53.4324	True
M2-Normal Water	M3-Normal Water	5.4	0.0	2.3676	8.4324	True
M2-Normal Water	M4-Autoclave curing	89.7	0.0	86.6676	92.7324	True
M2-Normal Water	M4-Boil water curing	22.4	0.0	19.3676	25.4324	True
M2-Normal Water	M4-Hot air curing	72.52	0.0	69.4876	75.5524	True
M2-Normal Water	M4-Normal Water	12.6	0.0	9.5676	15.6324	True
M3-Autoclave curing	M3-Boil water curing	-54.0	0.0	-57.0324	-50.9676	True
M3-Autoclave curing	M3-Hot air curing	-12.6	0.0	-15.6324	-9.5676	True
M3-Autoclave curing	M3-Normal Water	-57.6	0.0	-60.6324	-54.5676	True

M3-Autoclave curing	M4-Autoclave curing	26.7	0.0	23.6676	29.7324	True
M3-Autoclave curing	M4-Boil water curing	-40.6	0.0	-43.6324	-37.5676	True
M3-Autoclave curing	M4-Hot air curing	9.52	0.0	6.4876	12.5524	True
M3-Autoclave curing	M4-Normal Water	-50.4	0.0	-53.4324	-47.3676	True
M3-Boil water curing	M3-Hot air curing	41.4	0.0	38.3676	44.4324	True
M3-Boil water curing	M3-Normal Water	-3.6	0.0075	-6.6324	-0.5676	True
M3-Boil water curing	M4-Autoclave curing	80.7	0.0	77.6676	83.7324	True
M3-Boil water curing	M4-Boil water curing	13.4	0.0	10.3676	16.4324	True
M3-Boil water curing	M4-Hot air curing	63.52	0.0	60.4876	66.5524	True
M3-Boil water curing	M4-Normal Water	3.6	0.0075	0.5676	6.6324	True
M3-Hot air curing	M3-Normal Water	-45.0	0.0	-48.0324	-41.9676	True
M3-Hot air curing	M4-Autoclave curing	39.3	0.0	36.2676	42.3324	True
M3-Hot air curing	M4-Boil water curing	-28.0	0.0	-31.0324	-24.9676	True
M3-Hot air curing	M4-Hot air curing	22.12	0.0	19.0876	25.1524	True
M3-Hot air curing	M4-Normal Water	-37.8	0.0	-40.8324	-34.7676	True
M3-Normal Water	M4-Autoclave curing	84.3	0.0	81.2676	87.3324	True
M3-Normal Water	M4-Boil water curing	17.0	0.0	13.9676	20.0324	True
M3-Normal Water	M4-Hot air curing	67.12	0.0	64.0876	70.1524	True
M3-Normal Water	M4-Normal Water	7.2	0.0	4.1676	10.2324	True
M4-Autoclave curing	M4-Boil water curing	-67.3	0.0	-70.3324	-64.2676	True
M4-Autoclave curing	M4-Hot air curing	-17.18	0.0	-20.2124	-14.1476	True
M4-Autoclave curing	M4-Normal Water	-77.1	0.0	-80.1324	-74.0676	True
M4-Boil water curing	M4-Hot air curing	50.12	0.0	47.0876	53.1524	True
M4-Boil water curing	M4-Normal Water	-9.8	0.0	-12.8324	-6.7676	True
M4-Hot air curing	M4-Normal Water	-59.92	0.0	-62.9524	-56.8876	True

The pairwise comparison among interactions shown in Table 6 reported that all combinations of mix ratio and curing condition differed significantly, underscoring the interdependency between them. Especially, mix ratios of M4 cured by autoclave exhibited the highest strength and were significantly stronger than all other treatment combinations ($p < 0.001$). Alternatively, mix M1 resulted in the lowest strength among others. The detailed contrast showed that intermediate combinations like hot air curing of mix M3 and autoclave curing of mix M2 differed significantly, further suggesting the importance of jointly optimizing mix design and curing condition.

790 **4.10 Environmental implications**

791 In this study, the compressive strength of Reactive Powder Concrete (RPC) was evaluated
792 under various curing conditions, including normal water curing, boiling water curing, hot air
793 curing, and autoclave curing. These curing methods had notable environmental implications,
794 particularly regarding carbon emissions, energy consumption, water usage, and lifecycle
795 impacts. Normal water curing involved no carbon emissions or energy use but required a
796 significant amount of water, raising sustainability concerns in arid regions. Additionally, it
797 demands longer curing durations. Boiling water curing, on the other hand, consumed less water
798 but is energy-intensive, although it reduced the required curing time. Hot air curing eliminated
799 the need for water but still requires energy to generate heat. Autoclave curing involved high
800 energy consumption and associated carbon emissions; however, it minimized water usage and
801 shortened curing time. Despite the environmental trade-offs, autoclave curing demonstrated the
802 highest compressive strength, followed by hot air curing. Autoclave curing offered potential
803 lifecycle benefits by producing highly durable concrete that may reduce the need for
804 maintenance and repair, thereby offsetting some environmental costs. Therefore, selecting a
805 curing method for RPC requires balancing mechanical performance with environmental impact.

806 The environmental implications of RPC are also significantly influenced by the materials
807 used in its composition. In this study, industrial by-products such as silica fume, Alccofine, and
808 copper slag were incorporated into the mix. These materials helped reduce the reliance on
809 cement, a major contributor to carbon emissions, while also diverting waste from landfills. Their
810 use lowered the overall carbon footprint of RPC and supported the principles of sustainable
811 construction. As a result, incorporating such waste materials not only mitigates environmental
812 impacts but also contributes to a circular economy. Overall, the combination of optimized curing
813 strategies and sustainable material use presented a viable path towards high-performance,
814 environmentally responsible RPC.

815

5. Conclusion

Cubes using four mix proportions of Reactive Powder Concrete were cast and tested for compressive strength under four curing conditions, such as normal water curing, boil water curing, hot air curing, and autoclave curing. In addition, water absorption, impact strength, water sorptivity, RCPT, residual compressive strength after elevated temperature exposure, and acid attack under autoclave curing were done. The statistical analysis ANOVA was done to prove the statistical significance of experimental results.

From the results, it was observed that both M4 and M3 had superior qualities, as they have more cementitious content compared to the others. However, to reduce carbon emissions, more cement content in M3 has to be reduced. Likely, M4, 10 % of cement was replaced by a processed industrial waste, alccofine, and 40 % of quartz sand was replaced with copper slag, emerging as the best. More studies need to be carried out regarding the impact of increasing these percentages. Also, this research concluded that autoclave curing is better than the other curing options for RPC. This conclusion was also supported by using ANOVA and Tukey's HSD post-hoc analysis. Also, ANOVA results showed that optimizing both curing condition and mix ratio is crucial for achieving a better-performing concrete. Finally, concrete made with an M4 mix ratio under autoclave curing will be durable, sustainable, and eco-friendly and will be suitable for ultra-high-strength applications such as bridges, dams, high-rise buildings, and offshore structures.

Despite the several advantages of using industrial waste materials in Reactive Powder Concrete (RPC), certain limitations still exist. Firstly, the particle size of industrial waste materials, mainly copper slag, varies depending on their source. However, the development of RPC requires ultra-fine particles to achieve ultra-high packing density. Therefore, these materials must be processed before being used in RPC production. Secondly, the physical and chemical composition of industrial waste materials also varies based on their source and manufacturing process, which can influence the performance of RPC. Although durability

studies have been conducted, long-term performance data such as creep and shrinkage and long-term aging behaviour under different environmental exposures are still limited, raising concerns about the lifecycle performance of RPC. Hence, a recommendation for further research is to address these limitations, with a particular focus on long-term performance, environmental safety, and large-scale implementation for sustainable concrete production. Here, the mix proportions were determined by using the trial and error method, but in future research, it can be optimized by using a statistical optimization technique such as the Taguchi method or response surface methodology to achieve improved performance and efficiency.

Acknowledgements

The authors express their sincere gratitude to the management and respected Principal of Mepco Schlenk Engineering College (MSEC), Sivakasi, for providing the necessary facilities to carry out this research work. Special thanks are extended to Dr. K. Babukannan, former Head of the Department of Civil Engineering, MSEC, for reviewing the preliminary draft of the manuscript and providing valuable suggestions. The authors also gratefully acknowledge Dr. S. D. Jenifer, Department of Mathematics, MSEC, for her timely and active support in performing the statistical analysis (ANOVA). We especially appreciate the dedicated assistance provided by Ms. R. Harshani (MSEC) during the experimental work.

References

- Abd El Raheem, A. H., Mahdy, M. I., & Abdel-Fattah, A. I. (2020), Properties of Reactive Powder Concrete with Various Water to Cement Ratios, Silica Fume, and Steel Fibres Contents, *IOSR Journal of Mechanical and Civil Engineering (IOSR-JMCE) e-ISSN*, ***17***(5), 41-64.
- Abed, M., & Nemes, R. (2019), Mechanical properties of recycled aggregate self-compacting high strength concrete utilizing waste fly ash, cellular concrete and perlite powders, *Periodica Polytechnica Civil Engineering*, ***63***(1), 266-277.
- Abid, M., Zeb, S., Shah, M. K., Muhammad, S., Bashir, M. O., Almujibah, H., & Onyelowe, K. C. (2025), Enhancing Mechanical Performance and Microstructure of Reactive Powder Concrete through Optimization of High-Temperature Curing Regimes, *Case Studies in Construction Materials*, **23**, e05069.
- Ahmed, A. (2024), Assessing the effects of supplementary cementitious materials on concrete properties: a review, *Discover Civil Engineering*, ***1***(1), 145.
- Al Biajawi, M. I., Embong, R., Muthusamy, K., Ismail, N., & Obianyo, I. I. (2022), Recycled coal bottom ash as sustainable materials for cement replacement in cementitious Composites: A review, *Construction and Building Materials*, ***338***, 127624.
- ASTM C1202-22, Standard Test Method for Electrical Indication of Concrete's Ability to Resist Chloride Ion Penetration, ASTM International, 2022.
- ASTM C1585-20, Standard Test Method for Measurement of Rate of Absorption of Water by Hydraulic-Cement Concretes, ASTM International, 2020.
- Atlı, I., & Ipek, M. (2024), Investigation of the Mechanical Behaviors of Sustainable Green Reactive Powder Concrete Produced Using Ferrochrome Slag and Waste Fiber, *Sustainability*, ***16***(11), 4714.

- Aygörmez, Y., Canpolat, O., Al-Mashhadani, M. M., & Uysal, M. (2020), Elevated temperature, freezing-thawing and wetting-drying effects on polypropylene fibre reinforced metakaolin based geopolymer composites, *Construction and Building Materials*, ***235***, 117502.
- Banerji, S., Al Sarfin, M. A., Sorensen, A. D., & Mountain-Plains Consortium. (2024), Durability and Volumetric Stability of Non-Proprietary Ultra High Performance Concrete Mixes Batched With Locally Sourced Materials (No. MPC-695), *Mountain-Plains Consortium*.
- Chen, G., Huang, Y., Yang, R., Yu, R., Xiao, R., Wang, Z., & Bao, M. (2023), Comparative study on mechanical properties and microstructure development of ultra-high performance concrete incorporating phosphorous slag under different curing regimes. *Construction and Building Materials*, **392**, 131963.
- Chen, X., Wan, D. W., Jin, L. Z., Qian, K., & Fu, F. (2019), Experimental studies and microstructure analysis for ultra high-performance reactive powder concrete, *Construction and Building Materials*, ***229***, 116924.
- Durai, T. N. P., Kandasamy, S., & Christabel, A. R. S. (2025), Enhanced Mechanical Properties in Green Concrete through Innovative Blends of GGBFS, Alccofine, and Metakaolin, *Hybrid Advances*, **11**, 100520.
- Fallah-Valukolaee, S., Mousavi, R., Arjomandi, A., Nematzadeh, M., & Kazemi, M. (2022), A comparative study of mechanical properties and life cycle assessment of high-strength concrete containing silica fume and nanosilica as a partial cement replacement, *Structures*, ***46***, 838-851.
- Feng, H., Zhang, Y., Xin, H., Zhao, J., & Shah, S. Y. (2025), Restrained Shrinkage in Ultra-High-Performance Concrete (UHPC)-Normal Strength Concrete Interface, *Journal of Building Engineering*, **111**, 113293.
- Gao, B., Xu, L., Tang, T., Su, K., Chi, Y., & Huang, L. (2024), Development of low-carbon ultra-high performance concrete with low cement content: Workability, mechanical properties, and microstructure characterization, *Journal of Building Engineering*, ***94***, 109907.
- Ge, L., Zhang, Y., Sayed, U., & Li, H. (2023), Study on properties of basalt fibre reinforcing reactive powder concrete under different curing conditions, *Journal of Materials Research and Technology*, ***27***, 5739-5751.
- Hameed, R., Tahir, M., Abbas, S., Sheikh, H. U., Kazmi, S. M. S., & Munir, M. J. (2024), Mechanical and durability characterization of hybrid recycled aggregate concrete, *Materials*, ***17***(7), 1571.
- Hasan, S. S. (2024), Effect of using waste fibers on the strength properties of sustainable reactive powder concrete, *Kufa Journal of Engineering*, ***15***(1), 95-107.
- Hendi, S. I., & Aljalawi, N. M. (2024), Effect of Various Curing Regimes on Some Properties of Reactive Powder Concrete RPC, *Journal of Engineering*, ***30***(11), 21-38.
- Hiremath, P. N., & Yaragal, S. C. (2017a), Effect of different curing regimes and durations on early strength development of reactive powder concrete, *Construction and Building Materials*, ***154***, 72-87.
- Hiremath, P. N., & Yaragal, S. C. (2017b), Influence of mixing method, speed and duration on the fresh and hardened properties of Reactive Powder Concrete, *Construction and Building Materials*, ***141***, 271-288.
- Hongthong, R., Tadang, C., Tangchirapat, W., & Jaturapitakkul, C. (2025), Influences of Steel Fiber Shapes and Contents on Compressive Strength, Shrinkage, and Creep of High Performance Concrete Containing High Volume Ground Bottom Ash, *Results in Engineering*, **26**, 105448.
- Huynh, T. P., Ngo, S. H., & Nguyen, V. D. (2024), A Modified Reactive Powder Concrete Made with Fly Ash and River Sand: An Assessment on Engineering Properties and Microstructure, *Periodica Polytechnica Civil Engineering*, ***68***(4), 1031-1039.
- IS 456:2000, Plain and Reinforced Concrete - Code of Practice, Bureau of Indian Standards, New Delhi.
- IS 516:1959, Methods of Tests for Strength of Concrete, Bureau of Indian Standards, New Delhi.
- IS 6461 (Part 7):1973, Glossary of Terms Relating to Cement Concrete, Part VII: Mixing, Laying, Compaction, Curing and Other Construction Aspects, Bureau of Indian Standards, New Delhi.
- IS:9013-1978, Method of making, curing and determining compressive strength of accelerated-cured concrete test specimens, Bureau of Indian Standards, New Delhi.
- Jalalinejad, M., Hemmati, A., & Mortezaei, A. (2023), Mechanical and durability properties of sustainable self-compacting concrete with waste glass powder and silica fume, *Periodica Polytechnica Civil Engineering*, ***67***(3), 785-794.
- Lessly, S. H., Kumar, S. L., Jawahar, R. R., & Prabhu, L. (2021), Durability properties of modified ultra-high performance concrete with varying cement content and curing regime, *Materials Today: Proceedings*, ***45***, 6426-6432.
- Mayhoub, O. A., Nasr, E. S. A., Ali, Y. A., & Kohail, M. (2021), The influence of ingredients on the properties of reactive powder concrete: A review, *Ain Shams Engineering Journal*, ***12***(1), 145-158.

- Mir, A. H., & Kumar, R. (2024), Experimental research on high strength concrete prepared by alccofine and polypropylene fiber, *Materials Today: Proceedings*.
- Mizani, J., Sadeghi, A. M., & Afshin, H. (2022), Experimental study on the effect of macro and microfibres on the mechanical properties of reactive powder concrete, *Structural Concrete*, ***23***(1), 240-254.
- Moolchandani, K. (2025), Industrial byproducts in concrete: A state-of-the-art review, *Next Materials*, ***8***, 100593.
- Mostofinejad, D., Nikoo, M. R., & Hosseini, S. A. (2016), Determination of optimized mix design and curing conditions of reactive powder concrete (RPC), *Construction and Building Materials*, ***123***, 754-767.
- Muhedin, D. A., & Ibrahim, R. K. (2023), Effect of waste glass powder as partial replacement of cement & sand in concrete, *Case Studies in Construction Materials*, ***19***, e02512.
- Nasr, M. S., Hasan, Z. A., Abed, M. K., Dhahir, M. K., Najim, W. N., Shubbar, A. A. F., & Habeeb, Z. D. (2021), Utilization of high volume fraction of binary combinations of supplementary cementitious materials in the production of reactive powder concrete, *Periodica Polytechnica Civil Engineering,* ***65***(1), 335-343.
- Naveed, M., Hameed, A., Rasool, A. M., Mukhtar, D., & Ahmed, T. (2025), AI-based non-linear models for mechanical and toughness properties of sustainable fiber-reinforced geopolymer concrete (FRGPC), *Mechanics of Advanced Materials and Structures*, ***32***(13), 3179-3203.
- Nguyen, T. N., Lowry, M., Tran, T. Q., Phadke, K., Bise, E., & Brand, A. S. (2025), Comparisons of Quarry By-Products as a Partial Replacement of Portland Cement in Pastes and Mortars, *CEMENT*, **21**, 100152.
- Nieświec, M., Niewiadomski, P., Sadowski, Ł., & Schroefl, C. (2025), Waste copper slag in special concrete: Current research and future applications, *Materials & Design*, **253**, 113970.
- Ojha, P. N., Singh, A., & Singh, B. (2021), Experimental investigations on substitution of natural sand in concrete with copper slag and blast furnace slag, *Journal of Asian Concrete Federation*, ***7***(1), 1-11.
- Pushpakumara, B. H. J., & Bandara, P. M. K. N. (2025), Evaluating the effectiveness of copper slag waste as a fine aggregate in concrete, *Construction and Building Materials*, **475**, 141046.
- Radhi, M. S., Rasoul, Z. M. A., & Alsaad, A. J. (2021), Mechanical behavior of modified reactive powder concrete with waste materials powder replacement, *Periodica Polytechnica Civil Engineering*, ***65***(2), 649-655.
- Rajasekar, A., Arunachalam, K., & Kottaisamy, M. (2018a), Durability of ultra high strength concrete with waste granite sand as partial substitute for aggregate, *Journal of Computational and Theoretical Nanoscience*, ***15***(2), 446-452.
- Rajasekar, A., Arunachalam, K., & Kottaisamy, M. (2019), Assessment of strength and durability characteristics of copper slag incorporated ultra high strength concrete, *Journal of Cleaner Production*, ***208***, 402-414.
- Rajasekar, A., Arunachalam, K., Kottaisamy, M., & Saraswathy, V. (2018b), Durability characteristics of Ultra High Strength Concrete with treated sugarcane bagasse ash, *Construction and Building Materials*, ***171***, 350-356.
- Raza, S. S., Ali, B., Noman, M., & Hussain, I. (2022), Development of reactive powder concrete with recycled tyre steel fibre, *Materialia*, ***22***, 101386.
- Raza, S. S., Qureshi, L. A., Ali, B., Raza, A., & Khan, M. M. (2021), Effect of different fibres (steel fibres, glass fibres, and carbon fibres) on mechanical properties of reactive powder concrete, *Structural Concrete*, ***22***(1), 334-346.
- Richard, P., & Cheyrezy, M. (1995), Composition of reactive powder concretes, *Cement and concrete research*, ***25***(7), 1501-1511.
- Rong, Q., Hou, X., & Ge, C. (2020), Quantifying curing and composition effects on compressive and tensile strength of 160–250 MPa RPC, *Construction and Building Materials*, ***241***, 117987.
- Sagar, B., & Sivakumar, M. V. N. (2021), Use of alccofine-1203 in concrete: review on mechanical and durability properties, *International Journal of Sustainable Engineering*, ***14***(6), 2060-2073.
- Salahaddin, S. D., Haido, J. H., & Wardeh, G. (2024), Rheological and mechanical characteristics of basalt fiber UHPC incorporating waste glass powder in lieu of cement, *Ain Shams Engineering Journal*, *15*(3), 102515.
- Salman, B. F., Al-Rumaithi, A., & Al-Sherrawi, M. H. (2018), Properties of reactive powder concrete with different types of cement, *International Journal of Civil Engineering and Technology IJCIET*, ***9***(10), 1313-21.

- Sebastin, S., Priya, A. K., Karthick, A., Sathyamurthy, R., & Ghosh, A. (2020), Agro waste sugarcane bagasse as a cementitious material for reactive powder concrete, *Clean Technologies*, ***2***(4), 476-491.
- Sevinc, A. H., & Durgun, M. Y. (2023), Elevated temperature performance of cementitious mortars containing pumice, barite, and basalt powder, *Journal of Building Engineering*, ***78***, 107552.
- Siddique, R. (2014), Utilization of industrial by-products in concrete, *Procedia Engineering*, ***95***, 335-347.
- Wu, H., Yao, P., Yang, D., Wang, C., Shen, J., & Ma, Z. (2022), Upcycling of construction spoil powder as partial cement replacement for sustainable cement-based materials: Properties and modification, *Journal of Cleaner Production*, ***369***, 133361.
- Yang, J., Zhu, J., Li, J., & Meng, R. (2024), Research progress on synthetic methods and application performances of polycarboxylic acids with different sequence structures, *Polymers for Advanced Technologies*, ***35***(1), e6190.
- Zhang, X., Wu, Z., Xie, J., Hu, X., & Shi, C. (2024), Trends toward lower-carbon ultra-high performance concrete (UHPC)–A review, *Construction and Building Materials*, ***420***, 135602.
- Zhang, Y., Wu, B., Wang, J., Liu, M., & Zhang, X. (2019), Reactive powder concrete mix ratio and steel fibre content optimization under different curing conditions, *Materials*, ***12***(21), 3615.